British Journal of Pharmacology (2005) 144, 840–848
www.nature.com/bjp

Blockade of HERG cardiac K^+ current by antifungal drug miconazole

[1]Kan Kikuchi, *,[1]Toshihisa Nagatomo, [1]Haruhiko Abe, [1]Kazunobu Kawakami, [2]Henry J. Duff, [3]Jonathan C. Makielski, [3]Craig T. January & [1]Yasuhide Nakashima

[1]Second Department of Internal Medicine, University of Occupational and Environmental Health Japan, Kitakyushu, Japan; [2]Department of Medicine, University of Calgary, Calgary, Alberta, Canada and [3]Department of Medicine, Section of Cardiovascular Medicine, University of Wisconsin, Madison, WI, U.S.A.

1 Miconazole, an imidazole antifungal agent, is associated with acquired long QT syndrome and ventricular arrhythmias. Miconazole increases the plasma concentration of QT-prolonging drugs by inhibiting the hepatic cytochrome *P*450 metabolic pathway, but whether it has direct effects on cardiac ion channels has not been elucidated.

2 To determine the mechanism underlying these clinical findings, we investigated the effect of miconazole on human *ether-a-go-go*-related gene (HERG) K^+ channels.

3 HERG channels were heterologously expressed in human embryonic kidney 293 (HEK293) cells and whole-cell currents were recorded using a patch-clamp technique (23°C).

4 Miconazole inhibited HERG peak tail current in a concentration-dependent manner (0.4–40 μM) with an IC_{50} of 2.1 μM ($n=3$–5 cells at each concentration, Hill coefficient 1.2). HERG block was not frequency-dependent. It required channel activation, occurred rapidly, and had very slow dissociation properties.

5 The activation curve was shifted in a negative direction ($V_{1/2}$: -9.5 ± 2.3 mV in controls and -15.3 ± 2.4 mV after 4 μM miconazole, $P<0.05$, $n=6$). Miconazole did not change other channel kinetics (activation, deactivation, onset of inactivation, recovery from inactivation, steady-state inactivation).

6 The S6 domain mutation, F656C, abolished the inhibitory action of miconazole on HERG current indicating that miconazole preferentially binds to an aromatic amino-acid residue within the pore-S6 region.

7 Our findings indicate that miconazole causes HERG channel block by binding to a common drug receptor, and this involves preferential binding to activated channels. Thus, miconazole prolongs the QT interval by direct inhibition of HERG channels.
British Journal of Pharmacology (2005) **144,** 840–848. doi:10.1038/sj.bjp.0706095
Published online 13 December 2004

Keywords: Miconazole; arrhythmia; ion channels; K^+ channel; membrane currents; long QT syndrome; HEK 293 cells

Abbreviations: HERG, human *ether-a-go-go*-related gene; I_{Kr}, rapidly activating component of the delayed rectifier K^+ current; I_{Ks}, slowly activating component of the delayed rectifier K^+ current; HEK, human embryonic kidney; DMSO, dimethyl sulphoxide; MiRP1, MinK-related peptide 1

Introduction

Miconazole is a widely prescribed imidazole antifungal drug available in topical, vaginal and parenteral formulas. Azole antifungals (e.g. fluconazole, ketoconazole) are associated with the acquired long QT syndrome and ventricular arrhythmias (Moss, 1999; Tonini *et al*., 1999; Wassmann *et al*., 1999; Dorsey & Biblo, 2000; Tamargo, 2000). Since azole antifungals inhibit multiple cytochrome *P*450 enzymes in the liver and gastrointestinal tract, the mechanism of arrhythmogenesis is considered to be a rise in the plasma concentration of QT-interval prolonging drugs (e.g., class III antiarrhythmic drugs, some H_1-receptor antagonists and antibiotics) that use the same metabolic pathway (Albengres *et al*., 1998; Venkatakrishnan *et al*., 2000; Roden, 2001). However, ventricular arrhythmia can occur in the absence of other QT-interval prolonging drugs (Coley & Crain, 1997; Wassmann *et al*., 1999), suggesting that azole antifungal drugs may have direct effects on the heart. In fact, ketoconazole has been reported to directly block human *ether-a-go-go*-related gene *(HERG or KCNH2)* encoded K^+ channels (Dumaine *et al*., 1998). Although miconazole is known to inhibit multiple cytochrome *P*450 enzymes (Venkatakrishnan *et al*., 2000; Zhang *et al*., 2002), it is not known whether miconazole exerts direct effects on HERG channels.

In mammalian cardiac ventricular cells, the principal repolarising currents activated during the action potential plateau are the rapidly (I_{Kr}) and slowly (I_{Ks}) activating components of the delayed rectifier K^+ current (Sanguinetti & Jurkiewicz, 1990; Carmeliet, 1993), with I_{Kr} encoded by

*Author for correspondence at: Second Department of Internal Medicine, University of Occupational and Environmental Health Japan, 1-1 Iseigaoka, Yahatanishi-ku, Kitakyushu 807-8555, Japan; E-mail: toshi@med.uoeh-u.ac.jp
Published online 13 December 2004

HERG (Curran *et al*., 1995; Sanguinetti *et al*., 1995; Trudeau *et al*., 1995). In addition to class III antiarrhythmic drugs, a remarkable array of structurally diverse therapeutic agents that cause acquired long QT syndrome block HERG or I_{Kr} channels (Viskin, 1999; Drici & Barhanin, 2000; Witchel & Hancox, 2000). One possible explanation for this is that these drugs bind to a common drug receptor within the pore of HERG channels. Using alanine scanning mutagenesis of the pore-S6 region of HERG channel, aromatic amino-acid residues (Y652 and particularly F656) were reported to be key determinants of drug binding to HERG channels (Mitcheson *et al*., 2000a).

The aim of the present study was to investigate the effect of miconazole on HERG K^+ channels heterologously expressed in a human cell line. We found that miconazole potently inhibited HERG K^+ current by preferential binding to activated channels with ultra-slow dissociation kinetics and that the binding required a common drug receptor within the pore-S6 region.

Methods

DNA constructs and transfection of HEK293 cells

HERG cDNA was subcloned into *Bam*HI/*Eco*RI sites of the pCDNA3 vector (Invitrogen, San Diego, CA, U.S.A.). HERG wild-type channels were stably expressed in a human embryonic kidney (HEK293) cell line as described previously (Zhou *et al*., 1998). The HERG F656C (phenylalanine to cysteine at position 656) mutation was generated by site-directed mutagenesis of wild-type HERG cDNA with the use of the QuikChange Site-Directed Mutagenesis Kit (Stratagene, La Jolla, CA, U.S.A.), and the integrity of the construct was verified by DNA sequencing. HEK293 cells were transfected with this construct using the lipofectamine method (Invitrogen). Stably transfected cells generated through G418 antibiotic selection were subcloned to achieve a uniform HERG expression level. The cells were cultured in Dulbecco's Modified Eagle's Medium (D-MEM: Life Technologies, Gaithersburg, MD, U.S.A.) supplemented with 10% fetal bovine serum, 100 U ml^{-1} penicillin and 100 μg streptomycin. For electrophysiological analysis, cells were harvested from the culture dish by trypsinisation, washed with D-MEM, and stored in this medium at room temperature for later use. Cells in culture dishes were easily detached by trypsinisation and studied within 8 h of harvest.

Electrophysiological recordings

HERG channel current was recorded using the whole-cell patch-clamp technique. Transfected cells were transferred to a bath mounted on the stage of an inverted microscope (Diaphot, Nikon, Japan). The bath was perfused with 4-(2-hydroxyethyl)-1-piperazineethanesulphonic acid (HEPES)-buffered Tyrode solution containing (in mM) 137 NaCl, 4 KCl, 1.8 $CaCl_2$, 1 $MgCl_2$, 10 glucose, and 10 HEPES (pH 7.4). The volume of the bath was 0.6 ml and the external solution in the bath was almost completely exchanged within 1 min at a perfusion rate of 1.25 ml min^{-1}. The internal pipette solution contained (in mM) 130 KCl, 1 $MgCl_2$, 5 ethylene glycol bis (beta-aminoethyl ether)-*N*,*N*,*N*′,*N*′-tetraacetic acid (EGTA), 5 Mg-ATP, and 10 HEPES (pH 7.2). Electrodes were constructed from borosilicate glass using a micropipette puller (P-87, Sutter Instrument Co., Novato, U.S.A.) and heat-polished with a microforge (MF-83, Narishige, Tokyo). The final resistance of the electrode was 3–5 MΩ when filled with the pipette solution. Membrane currents were recorded with an Axopatch 200B amplifier (Axon Instruments, Union City, U.S.A.) and digitised at 2–10 kHz with an analogue-to-digital converter (DigiData 1200B; Axon Instruments). Computer software (pCLAMP Ver. 8.1, Axon Instruments) was used to generate voltage clamp protocols, acquire data and analyse current traces. All experiments were performed at room temperature (23 $\pm$ 1°C).

Chemicals

Miconazole was kindly provided by the Mochida Pharmaceutical Co. (Tokyo) and was dissolved in dimethyl sulphoxide (DMSO) to prepare a stock solution (40 mM). Final drug concentrations were prepared by diluting stock solution with Tyrode solution. The highest concentration of DMSO used in this study was 0.1%. In preliminary experiments, HERG tail current amplitudes expressed in HEK293 cells were not significantly changed after 3 min of DMSO application at 0.1% ($n = 4$).

Statistical analysis

Data are expressed as mean $\pm$ s.e.m. Where applicable, n represents the number of cells studied. Statistical significance was analysed using a two-tailed Student's t-test (paired or unpaired). P-values < 0.05 were considered statistically significant. Curve fitting was performed using multiple nonlinear least-squares regression analysis (pCLAMP Ver. 8.1, Axon Instruments or Sigma Plot Ver. 7.0, SPSS Science, Chicago, IL, U.S.A.).

Results

Miconazole inhibits HERG channels expressed in HEK293 cells

The effect of miconazole on the HERG current–voltage (I–V) relationship is shown in Figure 1. HERG current was elicited from a holding potential of −80 mV by 4-s long depolarising steps to between −70 and 60 mV applied in 10 mV increments every 15 s. Tail current was recorded with a step to −50 mV for 6 s. Representative currents recorded in control conditions and 3 min after application of miconazole (4 μM) in the same cell are shown in Figure 1a. Miconazole reduced HERG current amplitude during the depolarising step as well as tail current. The averaged normalised I–V relationships for HERG current measured at the end of the depolarising steps and for peak tail current are shown in Figure 1b and c, respectively. Control HERG current during the depolarising steps was maximal at about 0–10 mV, with tail current fully activated following steps to 10–20 mV. Miconazole (4 μM) reduced the steady-state current amplitude to 25.2 $\pm$ 1.9% ($n = 6$) of control at 10 mV, and tail current peak amplitude to 27.8 $\pm$ 2.4% ($n = 6$) of control at 20 mV, respectively. Voltage-dependence of activation was also evaluated by plotting normalised tail current as a function of voltage. Data were fitted with a Boltzmann

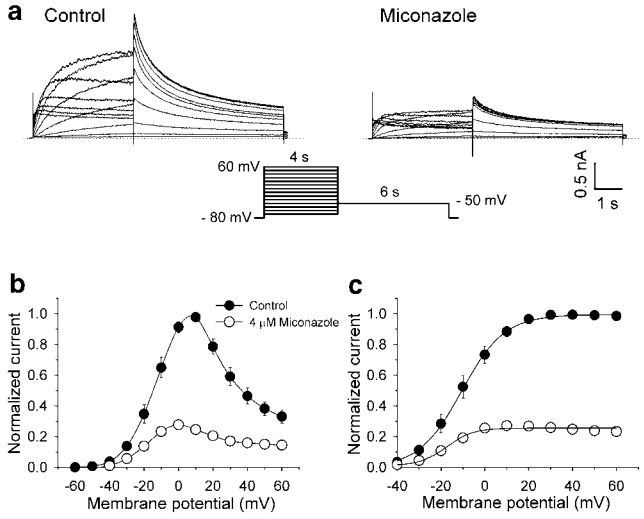

Figure 1 Current–voltage relationship for HERG channels and blockade by miconazole. (a) HERG currents under control conditions and in the presence of 4 μM miconazole recorded using the pulse protocol are shown. (b and c) Normalised (to respective control values) *I–V* relationships for current measured at the end of depolarising steps (b) and tail currents (c) in the control and the presence of 4 μM miconazole ($n=6$). Solid lines represent fits to Boltzmann function.

function: $I = I_{max} \times [1 + \exp(V_{1/2} - V)/\kappa]^{-1}$, where I_{max} is maximum amplitude, $V_{1/2}$ and κ are half-activation voltage and the slope factor, respectively. In this protocol, the half-activation voltage was significantly shifted in a negative direction from -9.5 ± 2.3 mV in controls to -15.3 ± 2.4 mV after miconazole ($P<0.05$, $n=6$) and the slope factor was significantly decreased from 8.7 ± 0.7 in controls to 6.9 ± 0.4 after miconazole ($P<0.05$, $n=6$).

Figure 2a shows the effects of miconazole (40 μM) on the HERG current during a drug wash-in protocol. HERG current was elicited from a holding potential of -80 mV by a 4-s depolarising step to 20 mV followed by a repolarising step to -50 mV for 6 s, and the protocol was applied every 15 s. After obtaining the control record, miconazole was applied to the bath. HERG channel block occurred rapidly to reach a steady-state level within 1–2 min (Figure 2b). The blocking effect on HERG channels was not reversed during washout of up to 10 min.

The concentration–response relationship of miconazole block was assessed by changes in the amplitude of HERG current measured at the end of depolarising step to 20 mV and the peak tail current after attaining steady-state drug block. Only a single drug concentration was tested on each cell. miconazole reduced HERG current in a concentration-dependent manner (Figure 2c). The IC_{50} value and Hill coefficient for HERG current measured at the end of depolarising step to 20 mV were 2.2 μM and 1.0, respectively, and for tail current peak amplitude were 2.1 μM and 1.2, respectively.

Attenuation of miconazole block by F656C mutant

Aromatic amino-acid residue, F656, located in the S6 transmembrane domain of HERG channels seem to play a major role in drug binding properties as reported previously (Mitcheson *et al*., 2000a). In order to gain additional

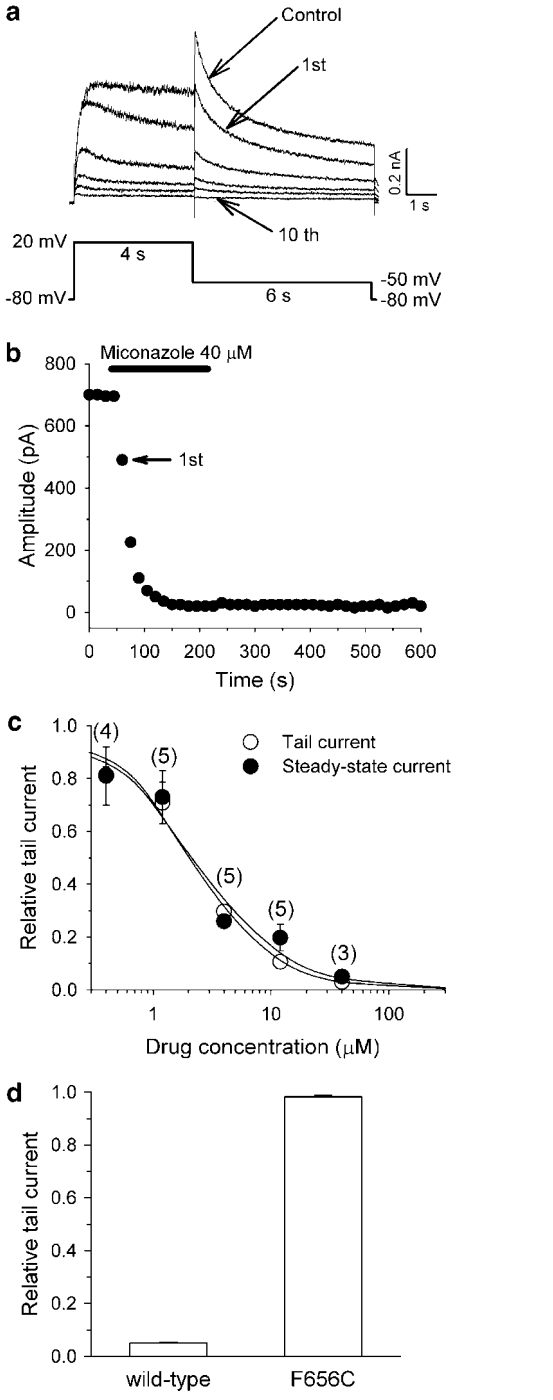

Figure 2 Miconazole inhibits HERG channels. (a) Representative current traces under control conditions and after application of miconazole (40 μM, the 1st, 2nd, 3rd, 4th and 10th current traces are shown). (b) Time course of miconazole-induced HERG tail current inhibition from the same cell shown in (a). (c) Concentration–response relationships for steady-state current amplitude measured at the end of depolarising step to 20 mV and peak tail current ($n=$ 3–5 cells at each concentration). Currents in the presence of miconazole were normalised to the control amplitudes and plotted as a function of drug concentration. Data represent the mean $\pm$ s.e.m. Numbers shown in parentheses indicate the number of cells tested. Solid lines represent fits with Hill equation: $I_{drug}/I_{control} = 1/[1 + (D/IC_{50})^n]$, where D is the drug concentration, IC_{50} is the drug concentration for 50% block, and n is the Hill coefficient. (d) Mean relative tail current amplitudes after application of 40 μM miconazole for HERG wild-type ($n=3$) and F656C mutant ($n=7$), respectively.

information on the molecular basis of miconazole binding to HERG channels, we investigated the effects of miconazole on HERG F656C mutant channels. The affinity of miconazole to HERG wild-type and mutant channels was compared by measuring the effects of miconazole at 40 μM (Figure 2d). Voltage protocols were applied as described in Figure 2a to record currents under control and after application of miconazole. In wild-type HERG channels, the tail current peak amplitudes were reduced to $5.0 \pm 0.3\%$ ($n=3$) of the control current amplitude (Figure 2c). The inhibitory effect of miconazole on HERG current was almost completely abolished in the F656C mutant channels. The mean relative peak amplitude of the tail current measured after 3 min of miconazole application yielded $98.2 \pm 0.6\%$ ($n=7$) of the control current amplitude.

State-dependence of HERG channel block by miconazole

To determine the state-dependence (closed, open and inactivated) of channel block, we used a protocol modified from Kiehn *et al*. (1996) and Thomas *et al*. (2001). From a holding potential of −80 mV, the cell was first depolarised to 80 mV for 100 ms to maximally activate channels from the closed state, and then the cell was repolarised to 0 mV for 300 ms to allow for maximal channel recovery from inactivated to the open state (see Figure 1). The cell was then either held at 0 mV (protocol 1) or a second step to 80 mV was applied for 300 ms to increase channel inactivation before step-back to 0 mV (protocol 2; Figure 3a). This approach of employing steps to very positive potentials was designed to determine whether maximal drug block occurred when channels were predominantly in the inactivated or open states. Figure 3a shows example control records with these protocols. With protocol 2 there was less current during the 300-ms long step to 80 mV because of increased channel inactivation, whereas following step-back to 0 mV, the current with both protocols was similar. Figure 3b shows the effect of miconazole (4 μM). For this experiment, cells were held continuously at −80 mV for 3 min during drug wash-in to keep the channels in the closed state. The data show that after drug wash-in, with the initial depolarisation a large amplitude HERG current was present consistent with minimal drug binding to the closed state, and this was followed by a decline in HERG current as drug block developed ('first pulse block'). The time-dependent decline in HERG current amplitude at 0 mV exhibited a single exponential process (dashed line). The 300-ms long step to 80 mV (protocol 2) interrupted this exponential time course and the current amplitude at the beginning of the second step to 0 mV exceeded the extrapolated predicted current amplitude by $7.9 \pm 1.3\%$ ($n=5$). The maximum current amplitude at the second step to 0 mV and the extrapolated predicted current amplitude at the same time point were 691 ± 184 and 645 ± 177 pA, respectively ($n=5$). The difference was statistically significant by the paired t-test ($P<0.01$). These results suggest that blockade by miconazole is weaker when the HERG channels are predominantly in the inactivated state. Thus, the block of HERG current by 4 μM miconazole requires channel activation from the closed state, and block is greater using protocols that maximise availability of open channels.

We examined in greater detail the possibility of closed state block. Using the protocol shown in Figure 3b, currents for control conditions and with first pulse block with 4 or 12 μM miconazole (Figure 3c and d, respectively) were superimposed for the initial step to 80 mV and the following step to 0 mV. With 4 μM miconazole, the initial current during the step to 80 mV was not different from the control current, and with the step to 0 mV block gradually developed, suggesting minimal closed state block (Figure 3c). When the drug concentration was increased to 12 μM (Figure 3d), a small reduction in the

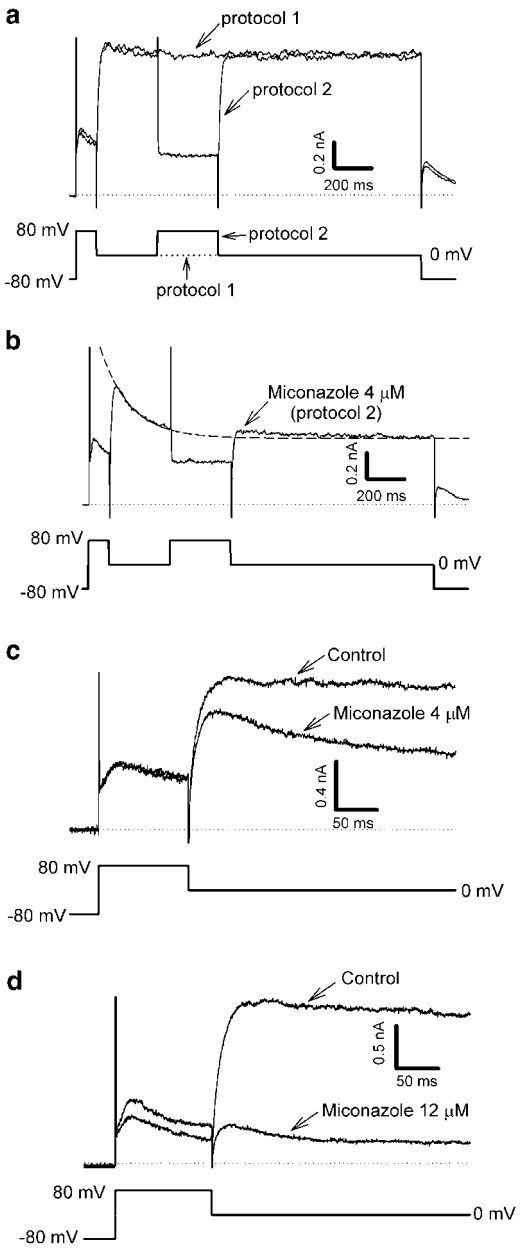

Figure 3 State-dependence of HERG channel block by miconazole. (a) Representative current recordings with a 300-ms long step to 80 mV (protocol 2) compared with a continuous step to 0 mV (protocol 1), see text for details. (b) First pulse current trace in the presence of miconazole (4 μM) with protocol 2. The current decay during the initial step to 0 mV was fitted with a single exponential function, which was extrapolated to the end of pulse protocol. The current amplitude at the beginning of the second step to 0 mV exceeded the extrapolated predicted current. (c and d) The initial current amplitude was not reduced by 4 μM miconazole but was reduced by 12 μM miconazole.

current amplitude was observed at the initial phase of the depolarisation step to 80 mV and there was greater block with the step to 0 mV, suggesting minor closed state block. However, the rapid development of open-channel blockade was not excluded, because drug binding might be accelerated at higher drug concentration. The peak current amplitudes evaluated at the initial 80 mV step-pulse were decreased by 5.4±2.9% ($n=5$) and 25.4±7.8% ($n=3$) after application of 4 and 12 μM miconazole, respectively ($P<0.05$). These results suggest that miconazole is predominantly an activated state blocker with higher affinity for the open state, and lowest affinity for the closed state.

Frequency dependence of HERG current block

The frequency dependence of HERG current block was investigated by applying 30 repetitive pulses (see inset, Figure 4) at 0.2 and 1 Hz, after holding the cell at −80 mV for 3 min during wash-in of 4 μM miconazole. HERG current was first rapidly activated by a 100 ms step to 80 mV, which was followed by a 400 ms step to 20 mV. As block of HERG current develops quickly after channel activation (see Figure 3), HERG current was measured as the maximum outward current amplitude during the step pulse at 20 mV, and was normalised to the control current measured prior to drug exposure. For control conditions, the HERG current amplitude during the pulse train decreased only slightly (<4%). Following exposure to 4 μM miconazole, application of the pulse train at either 0.2 or 1.0 Hz decreased current amplitude by 50.3±5.8% ($n=5$) at 0.2 Hz and by 51.1±2.4% ($n=5$) at 1 Hz. The time constants of the fast and slow components of the time course of block were not significantly different between the 0.2 and 1.0 Hz frequencies ($n=5$ cells at each pulsing rate). Thus, neither the development of block nor the amount of steady-state block was frequency-dependent.

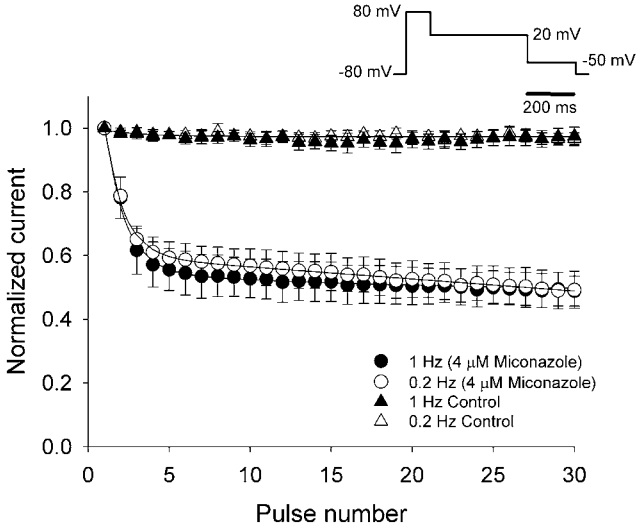

Figure 4 Inhibition of HERG tail current by miconazole is not frequency-dependent. After the cell was held at −80 mV for 3 min during exposure to 4 μM miconazole, 30 repetitive pulses (see inset) were applied at 1 and 0.2 Hz. HERG current amplitude measured as peak value during step to 20 mV for each pulse was normalised by the control peak current amplitude, and then plotted against the pulse number. For control conditions, there was little effect of the pulse train applied at 0.2 or 1 Hz ($n=5$), whereas in the presence of miconazole, HERG current was reduced similarly at 0.2 and 1.0 Hz pulse frequencies. Solid lines represent fits with double exponential function: $A_f\exp(-t/\tau_f)+A_s\exp(-t/\tau_s)+\text{base}$, where t is pulse number; τ_f and τ_s are time constants of fast and slow components; A_f and A_s are fractional amplitudes of fast and slow components. Fitting parameters were τ_f 1.16±0.12, τ_s 75.3±37.1 at 1 Hz ($n=5$) and τ_f 1.24±0.15, τ_s 64.7±17.8 at 0.2 Hz ($n=5$).

Effects of miconazole on kinetics of channel gating

Drug block of ion channels often exerts apparent effects on channel kinetics. Using voltage clamp protocols identical to those of Zhou *et al.* (1998), we measured activation, deactivation, inactivation and recovery from inactivation. After obtaining the control record, step pulses as illustrated in Figure 2a were applied in the presence of 4 μM miconazole for 3 min and then HERG current was recorded with identical protocols. To evaluate the time course of HERG channel activation, the cell was clamped to 20 mV from a holding potential of –80 mV for varying durations followed by a repolarising step to –50 mV to elicit tail current. The time constant obtained by fit to the envelope of tail currents was used for evaluation of the HERG current activation (Figure 5a and b). The time constants for activation did not significantly change after application of 4 μM miconazole (152±16 ms in control vs 141±17 ms after miconazole, $n=8$). Deactivation current was elicited by 10 mV step pulses from –100 mV to –20 ms after a 1-s depolarisation pulse to 60 mV from a holding potential of –80 mV (Figure 5c). Deactivation time constants were obtained by fit with double exponential function to the decay phase of tail current. The two time constants describing current decay were not significantly changed by 4 μM miconazole ($n=5$, Figure 5d).

To test the effects of miconazole on recovery from inactivation, the cells were depolarised to 60 mV for 200 ms to rapidly inactivate HERG channels and then repolarised to between –100 and –20 mV to elicit tail currents (Figure 6a). The rising phase of the tail current represents the rapid recovery of HERG channels from inactivated to open states. After fitting a double exponential function to the tail current trace at each potential, the time constant for the rising phase was used to measure recovery from inactivation. There was no significant difference before and after 4 μM miconazole application ($n=5$, Figure 6c).

We also studied the effects on the onset of inactivation with 4 μM miconazole. The cells were depolarised to 60 mV for 200 ms to promote inactivation and hyperpolarised to −100 mV for 10 ms, which is a sufficient time for recovery from inactivation as indicated in Figure 6c without significantly deactivating the channels (Figure 6b). Then, channels that recovered were forced to reinactivate at potentials between –20 and 60 mV. The time constant of inactivation was measured by fitting a single exponential function to the decaying current trace. The onset of inactivation was accelerated at strongly depolarised potentials (50 and 60 mV), but there were no significant differences between control and drug application in wide range of voltages ($n=5$, Figure 6c). Thus, miconazole has little effect on the rates of inactivation and recovery from inactivation of HERG channels.

Steady-state inactivation was measured using a double-pulse protocol with varying interpulse repolarisation levels

(Figure 6d). After the first 200 ms pulse to 60 mV promoting inactivation, 10 ms interpulses were applied to potentials between –100 and 20 mV, followed by a second step to 60 mV. Peak currents measured 3 ms after the onset of the second step to 60 mV were plotted as a function of the proceeding repolarising potential and then fitted with a Boltzmann function: $I = I_{max} \times [1-\exp(V-V_{1/2})/\kappa]^{-1}$, where I is current amplitude, I_{max} is maximum amplitude, $V_{1/2}$ and κ are half-inactivation voltage and the slope factor, respectively. Data from six cells under control and 4 μM miconazole were normalised to the asymptotic values of their respective Boltzmann fits (Figure 6e). The half-inactivation voltage and slope factor obtained by fit with Boltzmann equation were -64.8 ± 2.2 mV and -17.2 ± 1.3 in controls ($n = 6$), and -65.5 ± 1.4 mV and -17.2 ± 1.7 after 4 μM miconazole ($n = 6$), respectively. Both parameters were not statistically different. Thus, miconazole does not exert specific effects on channel inactivation. Otherwise unbinding upon repolarisation, which allows channels to become available for opening, does not occur because of the slow unbinding of miconazole from the channels and unchanged kinetics might reflect the kinetics of miconazole unbounded channels.

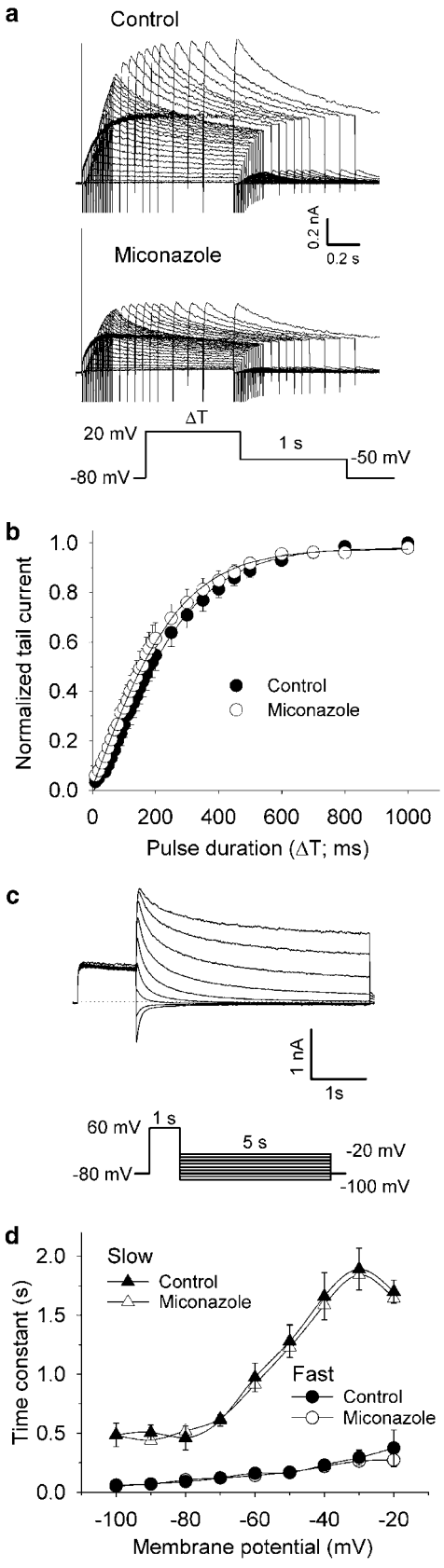

Discussion

In this study, we demonstrated that the azole antifungal drug miconazole potently inhibited HERG current heterologously expressed in a human cell line. As with most drugs, the block was state-dependent. Under our experimental conditions, closed (rested) state block was minimal and was noted only at high drug concentrations. In contrast, HERG channel block by miconazole required channel activation, and the greatest block appeared to be with the open state of the channel. As shown in Figure 3, evidence to support preferential open state block was derived from experiments showing a reduction in drug block at voltages (80 mV) where the occupancy of the inactivated state was greatest. Nevertheless, the experiments could not clearly distinguish between open or inactivated state block.

When trains of depolarising steps were applied, miconazole caused a progressive decrease in current, as expected for a drug with state-dependent block. The time course of development of block and the amount of steady-state block were not significantly different between 1.0 and 0.2 Hz (Figure 4). This lack of frequency-dependence can be accounted for by a very slow dissociation of the drug from the channel. With sufficiently slow drug dissociation the longer recovery interval between pulses at slower rates does not cause appreciable additional recovery over the time scale studied in our experiments. The negligible current recovery after drug

Figure 5 Effects of miconazole on activation time course and deactivation kinetics. (a) Representative current tracings for HERG current activation before and after application of 4 μM miconazole. Pulse protocol is shown in the inset. (b) The peak tail current after a repolarising step to –50 mV was plotted as a function of the test pulse duration (ΔT). Solid lines represent fits with a single exponential function. Data are expressed as mean ± s.e.m. ($n = 8$). (c) Representative current tracing for HERG current deactivation and pulse protocol (bottom inset). Deactivation time constants were obtained by fit with double exponential function to the decay phase of tail current. (d) Time constants for the deactivation are plotted against the membrane potential. Data are expressed as mean ± s.e.m. ($n = 5$).

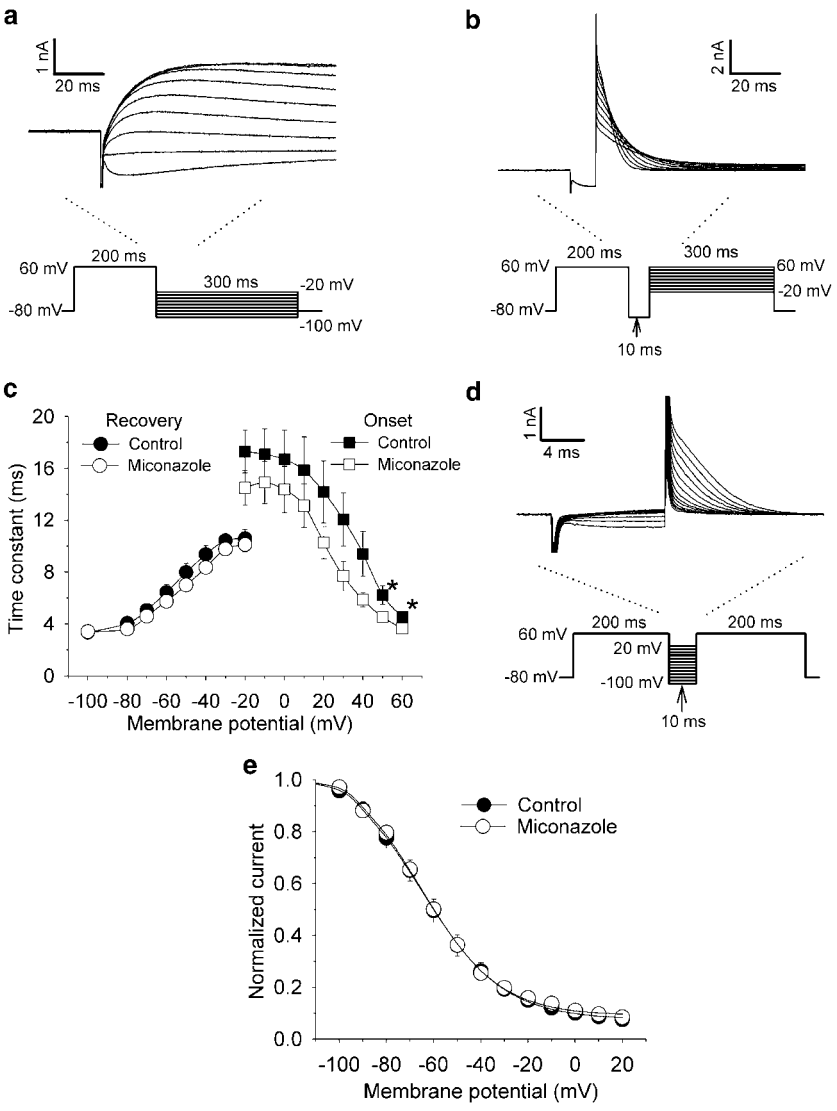

Figure 6 Effects of miconazole on inactivation kinetics. (a) Representative current tracing for HERG current recovery from inactivation elicited by the protocol shown below. Region of interest is magnified. After fitting to tail current with double exponential function, the time constant for the rising phase was used to evaluate the recovery. (b) Representative current tracing for HERG current onset of inactivation by using the protocol shown below. The time constants for the onset of inactivation were obtained by fitting exponential function to the decaying current traces during the third pulse of the protocol. (c) The time constants for the recovery and onset of inactivation are plotted against the membrane potential. Data are expressed as mean $\pm$ s.e.m. ($n=5$, $^*P<0.05$, control vs 4 μM miconazole). (d) Representative current tracing for steady-state inactivation by using a double-pulse protocol with varying interpulse repolarisation levels from -100 to 20 mV (bottom inset). (e) Normalised steady-state inactivation curves for control and after 4 μM miconazole application. Data are expressed as mean $\pm$ s.e.m. ($n=6$). Solid lines represent fits with Boltzmann function.

washout also supports the notion of very slow channel dissociation of this drug. The pattern of activated state block and slow dissociation is consistent with an activation gate trapping mechanism, as also reported for other HERG channel blocking drugs such as the methanesulphonanilide compounds (Carmeliet, 1992; Mitcheson *et al*., 2000b).

The structural basis of HERG channel block by several chemically unrelated compounds have recently been studied in detail. Aromatic amino-acid residues, particularly F656, located in the S6 transmembrane domain of HERG channels were proposed to be the most important molecular determinants of drug binding to HERG channels (Lees-Miller *et al*., 2000; Mitcheson *et al*., 2000a; Kamiya *et al*., 2001; Sanchez-Chapula *et al*., 2002; Scholz *et al*., 2003; Thomas *et al*., 2004). In the present study, F656C mutant channels markedly attenuated HERG current inhibition by miconazole. The result clearly shows that miconazole predominantly binds to a drug receptor within the pore-S6 region.

It is of interest to compare our findings with miconazole to previous findings with ketoconazole (Dumaine *et al*., 1998). Ketoconazole was reported to block HERG channels predominantly by binding to the closed state of HERG channels to cause tonic block, with lower affinity binding to the open state. In addition, HERG current block by ketoconazole was reversible upon drug washout. Our data show that block of HERG channels by miconazole required channel activation

from the closed state, and the drug block was not easily reversed by drug washout. Thus, miconazole appears to act like most drugs previously studied on HERG channels and I_{Kr}, where they bind preferentially to the channel following its activation from the closed state. The IC_{50} values for block of HERG tail current peak amplitude also differed (49 μM in ketoconazole (Dumaine *et al*., 1998), and 2.1 μM in miconazole). These differences may be attributed in part to differences in the expression systems used (*Xenopus* oocytes *versus* HEK293 cells), experimental conditions, and channel kinetics.

Clinical implications of HERG channel blockade by miconazole and limitations of the study

Although miconazole is associated with cardiac arrhythmias, the underlying mechanism(s) remains speculative. Since miconazole is known to inhibit multiple cytochrome *P*450 enzymes in the liver and gastrointestinal tract (Zhang *et al*., 2002), warnings have been issued against the concomitant administration of miconazole with QT interval-prolonging drugs that use the same metabolic pathway (Albengres *et al*., 1998; Venkatakrishnan *et al*., 2000; Roden, 2001). The present study demonstrates that miconazole also directly inhibits HERG channels. The maximal therapeutic concentrations of miconazole in patients ranges from 0.96 to 3.5 μg ml^{-1} when administrated intravenously, corresponding to 2.3–8.4 μM. Since the plasma protein binding for miconazole is reported to be approximately 90% (Stevens *et al*., 1976), the IC_{50} values determined in the present study may exceed slightly the expected free-drug concentration range in plasma. Thus, the apparent low incidence of QT prolongation by miconazole might in part be accounted for by its high protein binding. Nonetheless, our findings provide a direct cellular mechanism for miconazole-induced QT interval prolongation and cardiac arrhythmias. Direct inhibition of the HERG current may be of greater concern when miconazole is used in patients with congenital long QT syndrome, in patients with electrolyte abnormalities such as hypokalemia, or in patients receiving other QT interval prolonging drugs whether acting directly through HERG channel block or inhibition of drug metabolism through the *P*450 system.

The present study has certain limitations. We used HERG channels heterologously expressed in a human cell line. The possible effects of miconazole on other ion channels as well as receptors *in vivo* cannot be excluded. Secondly, minK-related peptide 1 (MiRP1), encoded by *KCNE*2, coassembles with the pore-forming HERG subunit and probably reconstitutes native I_{Kr} (Abbott *et al*., 1999). Compared to channels formed by the HERG subunit alone, HERG/MiRP1 complexes show altered channel properties and increase the potency of channel block by E-4031. Moreover, the mutant forms of MiRP1 demonstrated diminished potassium currents or increased channel blockade by drugs (Sesti *et al*., 2000). Therefore, it is possible that miconazole sensitivity might be different between HERG and HERG/MiRP1 channels, although wild-type MiRP1 does not markedly influence the drug sensitivity of the channels (Numaguchi *et al*., 2000; Kamiya *et al*., 2001; Scherer *et al*., 2002; Friederich *et al*., 2004).

We thank Drs Zhengfeng Zhou, Qiuming Gong, Brian P. Delisle and Blake D. Anson for expert technical assistance and advice. We thank Dr Shetuan Zhang for his review of the manuscript. This work was supported by Astrazeneca Research Grant (to T.N.), and by UOEH Research Grants for Promotion of Occupational Health (to T.N. and H.A.).

References

ABBOTT, G.W., SESTI, F., SPLAWSKI, I., BUCK, M.E., LEHMANN, M.H., TIMOTHY, K.W., KEATING, M.T. & GOLDSTEIN, S.A.N. (1999). MiRP1 forms I_{Kr} potassium channels with HERG and is associated with cardiac arrhythmia. *Cell,* **97,** 175–187.

ALBENGRES, E., LE LOUET, H. & TILLEMENT, J.P. (1998). Systemic antifungal agents. Drug interactions of clinical significance. *Drug Saf.,* **18,** 83–97.

CARMELIET, E. (1992). Voltage- and time-dependent block of the delayed K+ current in cardiac myocytes by dofetilide. *J. Pharmacol. Exp. Ther.,* **262,** 809–817.

CARMELIET, E. (1993). Mechanisms and control of repolarization. *Eur. Heart J.,* **14** (Suppl H), 3–13.

COLEY, K.C. & CRAIN, J.L. (1997). Miconazole-induced fatal dysrhythmia. *Pharmacotherapy,* **17,** 379–382.

CURRAN, M.E., SPLAWSKI, I., TIMOTHY, K.W., VINCENT, G.M., GREEN, E.D. & KEATING, M.T. (1995). A molecular basis for cardiac arrhythmia: HERG mutations cause long QT syndrome. *Cell,* **80,** 795–803.

DORSEY, S.T. & BIBLO, L.A. (2000). Prolonged QT interval and torsades de pointes caused by the combination of fluconazole and amitriptyline. *Am. J. Emergency Med.,* **18,** 227–279.

DRICI, M.D. & BARHANIN, J. (2000). Cardiac K^+ channels and drug-acquired long QT syndrome. *Therapie,* **55,** 185–193.

DUMAINE, R., ROY, M.L. & BROWN, A.M. (1998). Blockade of HERG and Kv1.5 by ketoconazole. *J. Pharmacol. Exp. Ther.,* **286,** 727–735.

FRIEDERICH, P., SOLTH, A., SCHILLEMEIT, S. & ISBRANDT, D. (2004). Local anaesthetic sensitivities of cloned HERG channels from human heart: comparison with HERG/MiRP1 and HERG/MiRP1 T8A. *Br. J. Anaesth.,* **92,** 93–101.

KAMIYA, K., MITCHESON, J.S., YASUI, K., KODAMA, I. & SANGUINETTI, M.C. (2001). Open channel block of HERG K^+ channels by vesnarinone. *Mol. Pharmacol.,* **60,** 244–253.

KIEHN, J., LACERDA, A.E., WIBLE, B. & BROWN, A.M. (1996). Molecular physiology and pharmacology of HERG. Single-channel currents and block by dofetilide. *Circulation,* **94,** 2572–2579.

LEES-MILLER, J.P., DUAN, Y., TENG, G.Q. & DUFF, H.J. (2000). Molecular determinant of high-affinity dofetilide binding to HERG1 expressed in Xenopus oocytes: involvement of S6 sites. *Mol. Pharmacol.,* **57,** 367–374.

MITCHESON, J.S., CHEN, J., LIN, M., CULBERSON, C. & SANGUINETTI, M.C. (2000a). A structural basis for drug-induced long QT syndrome. *Proc. Natl. Acad. Sci U.S.A.,* **97,** 12329–12333.

MITCHESON, J.S., CHEN, J. & SANGUINETTI, M.C. (2000b). Trapping of a methanesulfonanilide by closure of the HERG potassium channel activation gate. *J. Gen. Physiol.,* **115,** 229–240.

MOSS, A.J. (1999). The QT interval and torsade de pointes. *Drug Saf.,* **21** (Suppl 1), 5–10 ; discussion 81-87..

NUMAGUCHI, H., MULLINS, F.M., JOHNSON Jr, J.P., JOHNS, D.C., PO, S.S., YANG, I.C., TOMASELLI, G.F. & BALSER, J.R. (2000). Probing the interaction between inactivation gating and Dd-sotalol block of HERG. *Circ. Res.,* **87,** 1012–1018.

RODEN, D.M. (2001). Pharmacogenetics and drug-induced arrhythmias. *Cardiovasc. Res.,* **50,** 224–231.

SANCHEZ-CHAPULA, J.A., NAVARRO-POLANCO, R.A., CULBERSON, C., CHEN, J. & Sanguinetti, MC. (2002). Molecular determinants of voltage-dependent human ether-a-go-go related gene (HERG) K^+ channel block. *J Biol Chem.,* **277,** 23587–23595.

SANGUINETTI, M.C., JIANG, C., CURRAN, M.E. & KEATING, M.T. (1995). A mechanistic link between an inherited and an acquired cardiac arrhythmia: HERG encodes the IKr potassium channel. *Cell,* **81,** 299–307.

SANGUINETTI, M.C. & JURKIEWICZ, N.K. (1990). Two components of cardiac delayed rectifier K^+ current. Differential sensitivity to block by class III antiarrhythmic agents. *J. Gen. Physiol.,* **96,** 195–215.

SCHERER, C.R., LERCHE, C., DECHER, N., DENNIS, A.T., MAIER, P., FICKER, E., BUSCH, A.E., WOLLNIK, B. & STEINMEYER, K. (2002). The antihistamine fexofenadine does not affect I(Kr) currents in a case report of drug-induced cardiac arrhythmia. *Br. J. Pharmacol.,* **137,** 892–900.

SCHOLZ, E.P., ZITRON, E., KIESECKER, C., LUECK, S., KATHOFER, S., THOMAS, D., WERETKA, S., PETH, S., KREYE, V.A., SCHOELS, W., KATUS, H.A., KIEHN, J. & KARLE, C.A. (2003). Drug binding to aromatic residues in the HERG channel pore cavity as possible explanation for acquired Long QT syndrome by antiparkinsonian drug budipine. *Naunyn Schmiedebergs Arch. Pharmacol.,* **368,** 404–414.

SESTI, F., ABBOTT, G.W., WEI, J., MURRAY, K.T., SAKSENA, S., SCHWARTZ, P.J., PRIORI, S.G., RODEN, D.M., GEORGE Jr, A.L. & GOLDSTEIN, S.A. (2000). A common polymorphism associated with antibiotic-induced cardiac arrhythmia. *Proc. Natl. Acad. Sci. U.S.A.,* **97,** 10613–10618.

STEVENS, D.A., LEVINE, H.B. & DERESINSKI, S.C. (1976). Miconazole in coccidiodomycosis. II. Therapeutic and pharmacologic studies in man. *Am. J. Med.,* **60,** 191–202.

TAMARGO, J. (2000). Drug-induced torsade de pointes: from molecular biology to bedside. *Jpn. J. Pharmacol.,* **83,** 1–19.

THOMAS, D., HAMMERLING, B.C., WU, K., WIMMER, A.B., FICKER, E.K., KIRSCH, G.E., KOCHAN, M.C., WIBLE, B.A., SCHOLZ, E.P., ZITRON, E., KATHOFER, S., KREYE, V.A., KATUS, H.A., SCHOELS, W., KARLE, C.A. & KIEHN, J. (2004). Inhibition of cardiac HERG currents by the DNA topoisomerase II inhibitor amsacrine: mode of action. *Br. J. Pharmacol.,* **142,** 485–494.

THOMAS, D., WENDT-NORDAHL, G., ROCKL, K., FICKER, E., BROWN, A.M. & KIEHN, J. (2001). High-affinity blockade of human ether-a-go-go-related gene human cardiac potassium channels by the novel antiarrhythmic drug BRL-32872. *J. Pharmacol. Exp. Ther.,* **97,** 753–761.

TONINI, M., DE PONTI, F., DI NUCCI, A. & CREMA, F. (1999). Review article: cardiac adverse effects of gastrointestinal prokinetics. *Aliment. Pharmacol. Ther.,* **13,** 1585–1591.

TRUDEAU, M.C., WARMKE, J.W., GANETZKY, B. & ROBERTSON, G.A. (1995). HERG, a human inward rectifier in the voltage-gated potassium channel family. *Science,* **269,** 92–95.

VENKATAKRISHNAN, K., VON MOLTKE, L.L. & GREENBLATT, D.J. (2000). Effects of the antifungal agents on oxidative drug metabolism: clinical relevance. *Clin. Pharmacokinet.,* **38,** 111–180.

VISKIN, S. (1999). Long QT syndromes and torsade de pointes. *Lancet,* **354,** 1625–1633.

WASSMANN, S., NICKENIG, G. & BOHM, M. (1999). Long QT syndrome and torsade de pointes in a patient receiving fluconazole. *Ann. Intern. Med.,* **131,** 797.

WITCHEL, H.J. & HANCOX, J.C. (2000). Familial and acquired long qt syndrome and the cardiac rapid delayed rectifier potassium current. *Clin. Exp. Pharmacol. Physiol.,* **27,** 753–766.

ZHANG, W., RAMAMOORTHY, Y., KILICARSLAN, T., NOLTE, H., TYNDALE, R.F. & SELLERS, E.M. (2002). Inhibition of cytochromes *P*450 by antifungal imidazole derivatives. *Drug Metab. Dispos.,* **30,** 314–318.

ZHOU, Z., GONG, Q., YE, B., FAN, Z., MAKIELSKI, J.C., ROBERTSON, G.A. & JANUARY, C.T. (1998). Properties of HERG channels stably expressed in HEK 293 cells studied at physiological temperature. *Biophys. J.,* **74,** 230–241.

(Received September 28, 2004
Accepted November 10, 2004)